

Strain residual during hydraulic fracturing: an elastic model scenario with microseismicity

Neda, Boroumand and David, W., Eaton

Department of Geoscience, University of Calgary

Summary

We study the induced strain and stress regimes of an Earth model during hydraulic fracturing simulations. A three dimensional (3D) stress and flow numerical scheme is developed to study the microseismic observations with respect to deformation behavior. The simulated fracture in the Earth model is calibrated in time and space to the microseismic geometries. A geomechanical interpretation, through parameter selection, is performed to explain how the fractured region deformed. The strain residual model results show the areas of deformation and identify the subsurface parameters that caused the deformation.

Introduction

Microseismic events, symptomatic of induced hydraulic fractures, are used to characterize and image their growth patterns (Maxwell, 2011). Passive seismic monitoring systems are deployed in boreholes and/or on surface to record the events that occur in the destabilized regions surrounding the fractures. There have been several examples of geomechanical simulations and numerical illustrations tying microseismic event distributions to hydraulic fracturing (Guest, 2010 and Settari and Mourits, 1998). Fracture models are typically used to design treatment programs prior to executing the job in the field. But, a post-fracture interpretation which incorporates microseismic data, can yield valuable insights that could be used to improve and optimize future treatment design by understanding the subsurface parameters that influence fracture evolution.

When microseismic observations are used to constrain a geomechanical model, one can take full advantage of their interpretive potential. The purpose of numerical simulations is to run a number of deformation scenarios prior to conducting a treatment so that; 1) the ideal treatment can be designed that maximizes deformation, but limits fluid loss and unnecessary out of zone growth and 2) treatment plans can be revised to limit the potential for induced earthquakes. The following sections present the tools developed, analysis and evaluation approach recommended for microseismic interpretation. It particularly focuses on analysing the strain as part of characterizing the deformation process.

Theory and/or Method

There are many processes that occur during hydraulic fracturing and are presented schematically in Figure 1. This diagram depicts a tensile fracture, with a rectangular cross section that is forming in response to fluid injected at rate Q_{inj} . The blocky arrows indicate fluid that is entering the reservoir from the fracture. The pressurized bottom hole fluid creates a width, indicated as w_f , that grows as the internal fluid pressure overcomes the minimum horizontal in situ stress.

The tensile fracture, in Figure 1, creates a compressive zone surrounding the outside walls of the fracture, i.e. largest yellow oval. Within low permeability and compressible fluid filled reservoirs such as tight gas reservoirs, the microseisms, illustrated by yellow stars, are proximal to the hydraulic fracture (Cipolla, 2011). The leak off zone, shown by the transparent blue oval surrounding the fracture, is the region in the reservoir, outside of the fracture containing the fracture fluid that flowed across the fracture face. Depending on initial conditions, a porous rock with natural fractures may compress and dilate, due to stress

perturbations from the tensile fracture and/or fluid leakoff effects, thus causing near and far field anomalous microseismic activity.

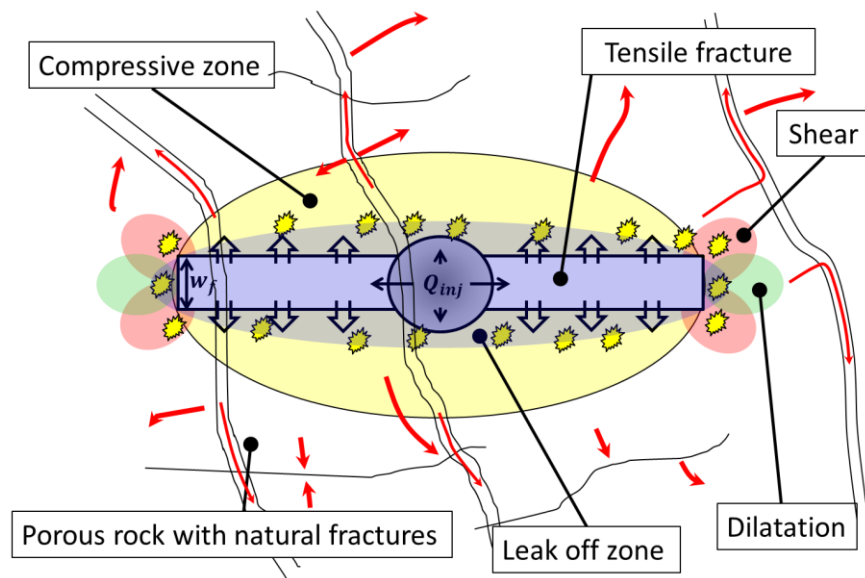


Figure 1 Map view schematic showing the physics of the fracturing process in a reservoir. The interactions include creation of hydraulic fracture, fluid injection and fluid flow, tensile fracture, generation of compression zone, shear lobes at fracture tips and fluid movement along natural fracture and throughout porous rock. Note that the microseismic events (yellow stars) are proximal to the hydraulic fracture in reservoirs with low permeability containing highly compressible fluid such as gas where leak off is limited.

Microseisms are interpreted to represent predominantly shear failure, and they occur commonly along preexisting or induced failure planes (Pearson, 1981; Warpinski et al., 2001) but can also exhibit a volumetric component (Valesco et al., 2014). They occur in theoretical zones of elevated compressive stress, as a result of pore pressure changes and formation strain and likely occur in zones of high shear stress associated with crack tip failure (Boroumand and Eaton, 2015). As such, the distribution of microseismic events is assumed to delineate the extent of the fracture, namely, the fracture half-length and half-height.

Shear stresses, indicated by pink lobes at either end of the rectangle (Figure 1) develop around the tips of the fracture as it propagates. Microseismic events also form in these areas of elevated shear stress, which provides a physical basis for why the fracture length and height, observed from microseismic maps can be used as a calibration tool in numerical models.

The numerical simulation using the coupled fluid and geomechanics code containing a fracture propagation criteria was run to evaluate the effects of input properties on fracture propagation. The example presented shows the sensitivity of the model results based on the selection of input parameters. These parameters were selected for the purposes of illustration and are not intended to represent a specific field example.

Examples

In previous previous work, we obtained the model parameters based on calibration of simulation and microseismic data (Boroumand and Eaton, 2015). In this example, we study the sensitivity of induced strain to the changes in model parameters for a symmetric and asymmetric example.

The algorithm developed for this study is well suited to handle subsurface complexities such as variations in stress, elastic and material properties. In this example, symmetric and asymmetric model profile for the input parameter, K_{IC} (i.e. fracture toughness), were adjusted to highlight predicted differences in the simulation results. This example shows the sensitivity of the model results based on the selection of input parameters. These parameters were selected for the purposes of illustration and are not intended to represent a specific field example.

The symmetric and asymmetric input models are shown in Figure 2 and Figure 3 respectively. To show a basic response, all other elastic, stress, material and fluid properties in both models are set to be homogeneous except the σ_{min} and K_{IC} parameters. Figure 2 and Figure 3 show that each model has defined an upper, target and lower layer. The target layer in the center has different values of σ_{min} and K_{IC} from the upper and lower layers. For the symmetric model, upper and lower layers have the same properties whereas, for the asymmetric model, the upper and lower layers have different K_{IC} values.

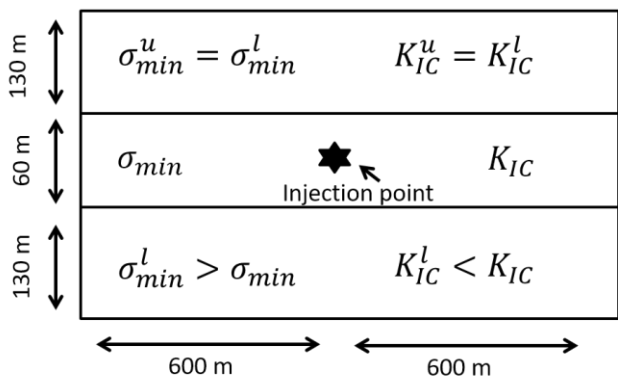


Figure 2 Symmetric geologic model with $\sigma_{min}^u = \sigma_{min}^l < \sigma_{min}$ and $K_{IC}^u = K_{IC}^l < K_{IC}$.

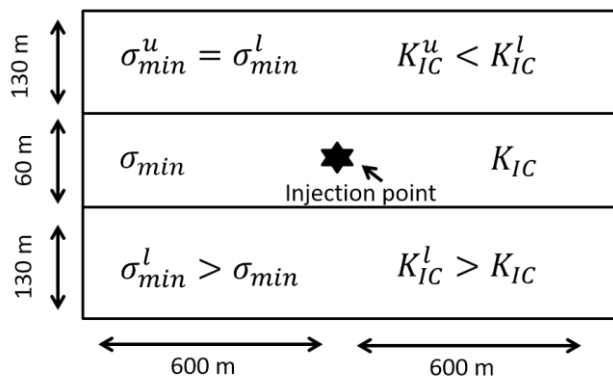


Figure 3 Asymmetric geologic model with $\sigma_{min}^u = \sigma_{min}^l < \sigma_{min}$ and $K_{IC}^u < K_{IC} < K_{IC}^l$.

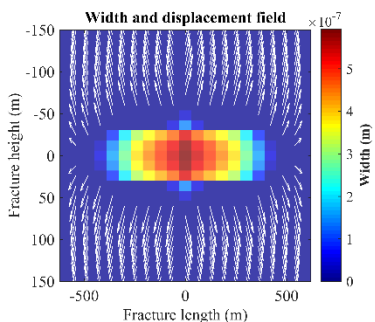


Figure 4 Symmetric width profile. The parameters chosen do not represent real field values, instead show the sensitivity of the model to the choice of parameter for a short run time. The white arrows represent the displacement at each lump around the exterior of the fracture.

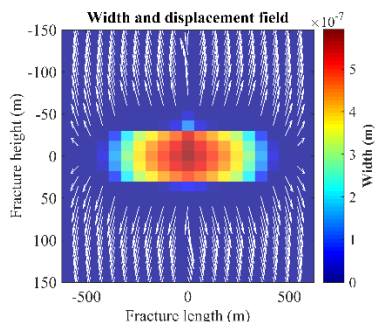


Figure 5 Asymmetric width profile. The parameters chosen do not represent real field values, instead show the sensitivity of the model to the choice of parameter for a short run time. The white arrows represent the displacement at each lump around the exterior of the fracture.

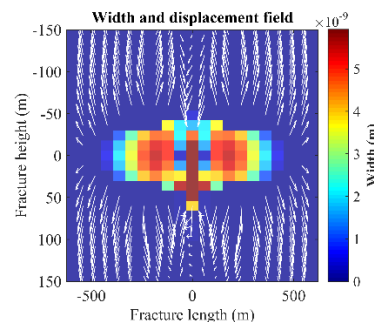


Figure 6 Symmetric minus asymmetric 2D displacement field height versus length overlain with width profile. The white arrows represent the difference in displacement, between the symmetric and asymmetric example at each lump around the exterior of the fracture. This visually shows by how much the displacement field was perturbed.

Figure 4 and Figure 5 compare the cross sectional view of the width profile of the propagated fracture for the symmetric and asymmetric cases respectively. The K_{IC} value for the lower layer in Figure 3 was increased to force the fracture to propagate in the target layer and up into the upper layer.

The cross-section view of the displacement field with respect to the fracture face are displayed in Figure 4 and Figure 5. The width of the opened fracture is represented using the background color scale. Automatic Gain Control (AGC) is applied to demonstrate the direction of displacement vectors (e.g white lines with arrows). The residual values of the displacement plots (white arrows) in Figure 6, highlight the sensitivity of the model response and where the largest changes in strain occur. The color plot shows the magnitude of the width created at each grid point.

These figures show that the numerical analysis of a three layer model produce an elliptical pattern along the width and length profile. This comparison suggests that in a realistic setting, the data are likely to exhibit greater complexity compared to the models presented in this section.

Conclusions

Microseismic mapping has brought new capabilities in the way of characterizing fracture(s). A few of these advancements, mainly those developed and investigated in this study, are summarized below.

A 3D numerical simulation that includes fluid flow and stress/strain interactions, via a coupled numerical algorithm, permits a deeper understanding of the subsurface processes. When the physics of the problem is accounted for, then

The strain residual shows variations in displacement along the fracture profile after the input parameters were adjusted. When these areas are correlated to populations of high or low microseismic activity, it can reveal if whether or not the correct parameter was selected. The hypothesis here is that if there is a large population of microseismic activity, then the parameter selected in the model could show large strain residual.

Acknowledgements

Sponsors of the Microseismic Industry Consortium are thanked for their support of this work. We are particularly grateful for support from the Natural Sciences and Engineering Research Council of Canada (NSERC) and Chevron for their support of an Industrial Research Chair in Microseismic System Dynamics at the University of Calgary. We would also like to thank Nexen Energy ULC, Spectris plc (ESG solutions) for providing the data to conduct this research. We are also grateful for the many valuable discussions had with Hassan Khaniani, Norm Warpinski, Tony Settari and the various students and staff within the UofC and UofA group over the years.

References

- Boroumand, N. and Eaton, D. W., 2015, Energy-based hydraulic fracture numerical simulation: Parameter selection and model validation using microseismicity: *GEOPHYSICS*, 80(5), W33-W44.
- Cipolla, C. L., Mack, M. G., Maxwell, S. C. and Downie, R. C., 2011, A practical guide to interpreting microseismic measurements: January 1 2011. doi:10.2118/144067-MS.
- Guest, A. and J. Settari, A., 2010, Relationship between the hydraulic fracture and observed microseismicity in the Bossier sands, Texas: SPE 137936.

Pearson, C. The relationship between microseismicity and high pore pressures during hydraulic stimulation experiments in low permeability granitic rocks. *Journal of Geophysical Research: Solid Earth*, 86(B9):7855-7864, 1981. doi:10.1029/JB086iB09p07855.

Settari, A. and Mourits, F. M., 1998, A Coupled Reservoir and Geomechanical Simulation System: *SPE Journal* 50939.

Velasco, R., Chambers, K., and Wilson, S. The characterization of fracture mechanisms using a combination of surface microseismic imaging, microdeformation modelling, and downhole microseismic mapping: An examination of the value of moment tensor microseismic imaging. *Unconventional Resources Technology Conference (URTEC)*, 2014. doi:10.15530/urtec-2014-1920493.

Warpinski, N. R., Wolhart, S. L., and Wright, C. A. Analysis and prediction of microseismicity induced by hydraulic fracturing. *Society of Petroleum Engineers*, January 1 2001. doi:10.2118/71649-MS.